Role of excitation-induced shift in the coherent optical response of semiconductors

Justin M. Shacklette and Steven T. Cundiff*
JILA, University of Colorado and National Institute of Standards and Technology, Boulder, Colorado 80309
(Received 5 October 2001; revised manuscript received 12 March 2002; published 17 July 2002)

A transient four-wave-mixing signal is shown to arise from an excitation induced shift. In semiconductors, this signal can be comparable to or stronger than signals arising from saturation, local fields, or excitation induced dephasing. Calculations using modified optical Bloch equations show that multiple peaks in the transient four-wave-mixing spectrum are a signature of an excitation induced shift contributing to the signal. We observe this experimentally from a semiconductor multiple quantum well and confirm the presence of a shift directly using spectrally resolved differential transmission.

DOI: 10.1103/PhysRevB.66.045309 PACS number(s): 71.35.Cc, 42.50.Md

The interaction between light and semiconductors provides fundamental insight into the dynamics of the optically created excitations. This is particularly true when techniques that are sensitive to coherence are employed. Coherent spectroscopy is well understood for a dilute vapor, where only isolated atoms or molecules need to be considered.[1] In dense materials, such as semiconductors or a dense atomic vapor, many-body interactions lead to dramatic differences from the dilute limit.[2] These effects can completely alter the interpretation of spectroscopic measurements and the performance of optoelectronic devices.

Substantial progress has been made in understanding how interactions among elementary optical excitations (excitons or unbound electron-hole pairs) influence the coherent optical response of semiconductors, which is typically observed using transient four-wave mixing (TFWM). Early work[3–5] was interpreted based on the optical Bloch equations (OBE's),[6] which are appropriate in the dilute limit. Subsequently, it was realized that in addition to the signals arising from saturation, which are described by the OBE's, there were additional signals due to the interactions. The appearance of a signal for ''negative'' delay in a two-pulse TFWM experiment and a delay in the emission as a function of real time[7,8] are the most dramatic signatures. These effects can be calculated using a full many-body treatment.[9,10] In addition, they can be described phenomenologically in a few-level approach as arising from local fields,[11,12] excitation induced dephasing (EID),[13–15] and biexcitonic effects.[16,17] The phenomenological approach yields corrections to the OBE's, which can produce very good agreement with experiment[18] including complex polarization selection rules.[19] While the full many-body treatment is clearly based on a stronger theoretical foundation, the phenomenological description is usually easier to understand in terms of the underlying physics. The foundation provided by the full many-body treatment has been used to develop a microscopic basis for the phenomenological few level approach.[20]

We show that an excitation induced shift (EIS) can result in a TFWM signal similar to that produced by the other mechanisms listed above. EIS is a manifestation of fundamental many-body interactions that result in a modification of the excitonic frequency in the presence of an excited carrier population. While the presence of EIS in semiconductors is well known from differential absorption measurements,[21,22] the fact that it results in a coherent TFWM signal has only been noted in passing[15] and its contribution to the TFWM signal has not been identified, to the best of our knowledge. Due to the similarities between the time-integrated TFWM signal produced by local fields, EID, and EIS, it is difficult to determine which one is responsible for the emitted signal. In addition, quantum interference due to excitation of continuum states causes the time integrated signal to decay rapidly as a function of delay.[23–25] To overcome this, we spectrally resolve the signal and observe a splitting in the peak, although the absorption spectrum shows only a single peak. Numerical calculations using modified optical Bloch equations show that only EIS can result in such a split peak. This provides clear proof that EIS is responsible for an important contribution to the TFWM signal. The presence of EIS is confirmed by performing spectrally resolved differential transmission (SR-DT) measurements, which provide characteristic line shapes that are distinct for saturation, EID, and EIS.

It is important to note that, although EID and EIS are ''excitation induced'' effects, the corresponding signals do not disappear in the low excitation density limit. This is because, for sufficiently low excitation density, the relevant parameter (dephasing rate or oscillation frequency) can simply be written as a linear function of the excitation density. As we see below in Eq. (2), the signal strength simply depends on the slope of the dephasing rate or oscillation frequency with excitation density, which is a constant. Contrary to intuition, these effects can actually be weaker at high excitation density because the change in the dephasing rate or oscillation frequency saturates due to screening and other many-body interactions. Wang *et al.* discussed this point with respect to the excitation dependent polarization properties of the EID signal and the excitation dependence of the dephasing rate.[13] Although the signal due to EIS and EID may dominate and have a cubic dependence for sufficiently low excitation density, the spectrum of the signal can still depend on excitation density.

The full many-body theory of the coherent response of semiconductors provides a good microscopic model that reproduces the experimentally observed TFWM signal if correlation terms beyond the mean field are included, up to sixth-order correlations have clearly been identified.[26] These correlation terms collectively described the phenomena of biexcitonic correlations, EID, and EIS. In many-body language, the latter two are due to renormalization of the self-

energy, with EIS corresponding to the real part and EID the imaginary part. Thus care is needed to unravel how these contribute to the TFWM signal based on a many-body model. As a consequence, the nature of these higher-order correlations are not fully understood and further research is required.[2]

Split peaks or dips at the exciton energy have been observed several times in spectrally resolved TFWM signals from ZnSe quantum wells. It was attributed to the presence of antibound states,[27] and interference between coherent and incoherent contributions.[28] Line shapes very similar to those we present below were attributed to reabsorption in a five quantum well sample[29] and an optically thick single quantum well.[30] To reduce the effect of reabsorption, further experiments were performed on optically thin single quantum wells by the latter group.[31] A dip at the heavy-hole (hh) line center was still observed for a specific polarization configuration and attributed to contributions from the two-pair continuum.[31] This work also observes that the spectral position of the exciton peak shifts as a function of delay, which is reproduced in the theory that includes the pair continuum contributions. None of this prior work discusses EIS or how it directly causes a contribution to the TFWM. Presumably such contributions are present in the many-body theory used to model the experiments as part of the self-energy renormalization, however, the real and imaginary parts are not distinguished. Thus our results can also contribute to a better understanding of the many-body effects. We note that all of the results from ZnSe show two peaks due to the presence of strong biexciton contributions. This results in an apparent ''split'' spectrum, however, the underlying physics is completely different from what we discuss here.

The fact that we observe a spectral dip for the common configurations of collinear and cocircular polarized incident pulses is an important distinction between our work and that on optically thin ZnSe quantum wells where the dip is only observed for the special case of where the first pulse is σ^+ polarized and the second pulse is linear polarized in the x direction.[31] We attribute the fact that we observe a dip in all cases to a substantial population of free carriers that are excited by the broad band incident pulses. In addition to increasing the excitonic dephasing rate, free carriers cause a stronger shift of the excitonic resonance frequency than a population of excitons alone. In ZnSe and other wide-gap materials where the excitonic binding energy is much larger, broadband pulses predominantly create excitons. Thus the effects that we observe, which are stronger in the presence of free carriers, would have been weak in those experiments. These differences in excitation conditions account for the differing polarization configurations and other parameters for which a split peak is observed in our experiment as compared to prior work. Additionally, our cocircular results rule out biexcitonic effects.

EIS can also occur in systems other than semiconductors. Evidence for EIS has been observed in a dense atomic vapor due to the difference in collision cross section between excited and ground states.[32] It is also similar to excited state shifts in molecular systems.[33] Thus EIS must be considered when analyzing the TFWM signals from these systems as well.

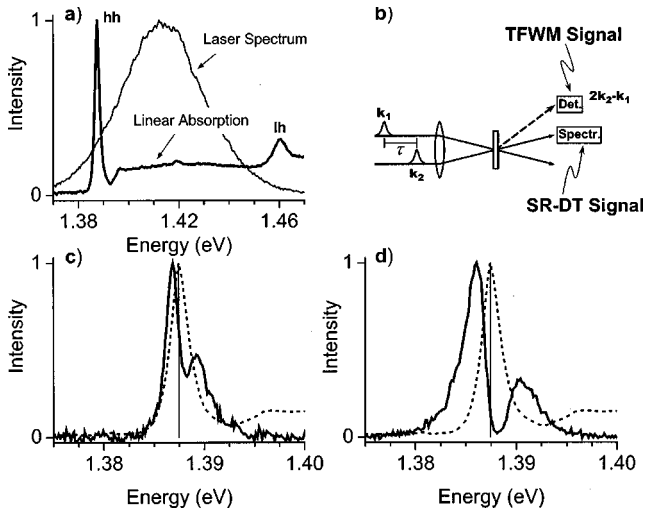

FIG. 1. (a) Linear absorption and laser spectrum. Experimental setup (b) shows the two-pulse configuration for TFWM and DT in transmission. Typical SR-TFWM data, in transmission (c) and in reflection (d), both for $\tau=0$ delay. The dashed lines in (c) and (d) show the linear absorption spectrum.

We studied a 50-period multiple quantum well structure of 8.3-nm-thick $In_{0.14}Ga_{0.86}As$ wells and 8.0-nm-thick $GaAs_{0.71}P_{0.29}$ barriers.[34] The quantum well layers are symmetrically strained, which increases the heavy hole (hh)–light hole (lh) splitting to 70 meV. This allows broadband excitation of the hh and the continuum, while avoiding band mixing between the hh and the lh. The binding energy for the hh exciton is approximately 4 meV. All measurements were carried out with the sample held at 8 K in a cold finger cryostat. Using a Kerr-lens-mode-locked Ti:sapphire laser,[35] the sample is illuminated with pulses from 10 to 40 fs in duration (corresponding to a transform limited bandwidth from 70 to 15 nm) at a repetition rate of 90 MHz. The laser is typically tuned to produce 40-fs pulses with a spectrum that overlaps the hh exciton and the continuum, but not the lh [see Fig. 1(a)].

The TFWM experiment was carried out in the standard two-pulse self-diffraction configuration as depicted in Fig. 1(b). In this configuration, the coherent signal is emitted in the direction $2\mathbf{k}_2-\mathbf{k}_1$, where $\mathbf{k}_1$ is the incident wave vector of the first pulse assuming the nominal time ordering, and $\mathbf{k}_2$ is the incident wave vector of the second pulse delayed by time τ. For all data presented here, the pulses are collinearly polarized in the plane defined by the wave vectors of the incident pulses. The TFWM signal is integrated temporally and spectrally by using a detector with a slow response compared to the time between pulses. To obtain additional information, we spectrally resolve the signal (SR-TFWM) using a $\frac{1}{4}$ meter spectrometer.

In Fig. 1(c), we show the SR-TFWM signal for zero delay (pulses temporally coincident) and low intensity excitation pulses. For comparison, the linear absorption is also shown. The spectrum has a pronounced dip at approximately the

center line. An obvious explanation for the dip is reabsorption of the TFWM signal as it propagates through the sample.[30] However, reabsorption is inconsistent with the slight shift between the center of the dip and peak of the linear absorption. To further rule this out, we performed the TFWM experiment in the reflection geometry [Fig. 1(d)], where the signal is emitted in the direction that is the reflection of $2\mathbf{k}_2$-$\mathbf{k}_1$ about the sample surface.[36] This shows that the dip is *stronger* in reflection than transmission, which is contrary to the expectation if the dip is due to reabsorption. Although reabsorption can affect the reflected signal, depletion of the incident pulses means that the first quantum wells will contribute more strongly to the signal than quantum wells that are deeper in the sample. However, the signal from the first quantum wells will experience stronger reabsorption in the transmission signal due to the remaining wells, than in reflection where there are no additional wells. The opposite is true for quantum wells deeper in the sample. Since depletion means that the signal from the first quantum wells provide a greater contribution to the total signal in either case, a dip due to reabsorption should have the opposite dependence from what we observed, namely it should be stronger in transmission than reflection. Therefore we conclude that the dip cannot be due to reabsorption alone. At the excitation densities ($\sim 5\times 10^9$ pairs/layer/cm^2) used for Figs. 1(c) and (d), the strength of signal is cubic with incident laser power. At higher excitation densities, the dip becomes less pronounced in both transmission and reflection geometries, although it is clearly no longer cubic. No significant change occurs as the incident intensity is lowered. However, due to the cubic intensity dependence of the signal on incident power, the input intensity can be reduced by only a factor of 2 before the signal to noise becomes sufficiently poor that any changes are obscured.

To examine other possible origins for the dip in the TFWM spectrum, we choose to use the phenomenological approach and solve the OBE's with corrections for local field, EID, and EIS. We ignore the biexciton contribution because the same spectrum is obtained for cocircularly polarized pulses, which prevent the formation of a bound biexciton since only opposite spin excitons can bind to form a biexciton. The corrected OBE's, which we call modified optical Bloch equations (MOBE's), are

$$\dot{\rho}_{22} = -\gamma\rho_{22} + \frac{i}{\hbar}[\mu_{12}(E+LP)](\rho_{12}-\rho_{21})$$

$$\dot{\rho}_{12} = -(\gamma_{ph}+\gamma' N\rho_{22})\rho_{12} + i(\omega_A+\omega' N\rho_{22})\rho_{12} + \frac{i}{\hbar}[\mu_{12}(E+LP)](\rho_{22}-\rho_{11}), \quad (1)$$

where ρ_{ij} are the elements of the density matrix with $\rho_{11}+\rho_{22}=1$, γ is the spontaneous emission rate, μ_{12} is the dipole matrix element, γ_{ph} is the dephasing rate, ω_A is the unexcited center frequency, E is the applied field, N is the density, and P is the polarization given by $P=N\,\mathrm{Tr}(\mu\rho)$. Phenomenological corrections for local field, EID, and EIS are included as L, γ', and ω' respectively.

Using perturbation theory with delta-function pulses, we analytically solve the MOBE's for the third-order polarization. The observed cubic dependence of the signal suggests that a third-order solution should be sufficient. Keeping only those terms in the direction $2\mathbf{k}_2$-$\mathbf{k}_1$ and neglecting coherent transients, the third-order polarization in the rotating wave approximation (RWA) is

$$\hat{P}_{12}^{(3)}(t) = i\frac{{\mu_{12}}^4}{\hbar^3}\frac{N}{8}E_2^2E_1^*\{[1+C(1-e^{-\gamma(t-\tau)})]e^{-\gamma_{ph}t} \times\Theta(t-\tau)\Theta(\tau)+C(1-e^{-\gamma t})e^{-\gamma_{ph}(t-2\tau)}\Theta(t) \times\Theta(-\tau)\}e^{+i(\omega_A-\Omega-\eta N)(t-2\tau)}+\text{c.c.}, \quad (2)$$

where $C=N(\gamma'-i2\eta-i\omega')/\gamma$, $\eta=\mu_{12}^2L/\hbar$, E_i is the electric-field strength of the pulse in direction $\mathbf{k}_i$, the first pulse arrives at time $t=0$, the second pulse arrives at time $t=\tau$, N is the initial ground-state population, and $\Theta(x)$ is the step function. The time integrated TFWM intensity is calculated by taking the absolute square of Eq. (2) and integrating over time, yielding

$$I_s(\tau) = \frac{{\mu_{12}}^8}{\hbar^6}\frac{N^2}{128}\frac{I_2^2I_1}{\gamma_{ph}}\left[\left(1+\frac{2\gamma' N}{\gamma+2\gamma_{ph}}\right)e^{-2\gamma_{ph}\tau}\Theta(\tau) + \frac{N^2[\gamma'^2+(2\eta+\omega')^2]}{(\gamma+2\gamma_{ph})(\gamma+\gamma_{ph})} \times(e^{-2\gamma_{ph}\tau}\Theta(\tau)+e^{+4\gamma_{ph}\tau}\Theta(-\tau))\right], \quad (3)$$

where I_i is the intensity of the pulse in direction $\mathbf{k}_i$. The first term in Eq. (3) is the signal due to saturation; it occurs only for $\tau>0$ and decays exponentially at a rate of $2\gamma_{ph}$. The second, third, and fourth terms in Eq. (3) all involve interactions and depend on the phenomenological parameters L, γ', and ω'. The fourth term is of particular interest because it is the only term present for $\tau<0$, thus a signature of complex interactions is a signal at negative delay. This perturbation result proves our prior statement that the signals due to EID and EIS do not disappear for arbitrarily low intensities, clearly decreasing the pulse intensities in this equation do not change the relative strength of the EID or EIS terms compared to the ordinary saturation term. Thus they can be the dominant signal for arbitrary low excitation density. The SR-TFWM signal is given by taking the Fourier transform of Eq. (2) and taking the modulo squared, which yields the spectral intensity. It is clear from Eq. (3) that EIS (terms with ω') is a TFWM signal that appears on an equal footing to EID (terms with γ'). The relative strength of the EID and EIS signals will be determined solely by relative sizes of γ' and ω'.

This perturbation result shows that EIS must be considered, but it does not show the split spectrum that we observe experimentally. Indeed the calculation does not even show the faster decay of the TFWM signal (and corresponding broadening of the spectrum) that must accompany EID. In previous treatments, this has been added "by hand."[15] This must be done carefully because populations can be generated

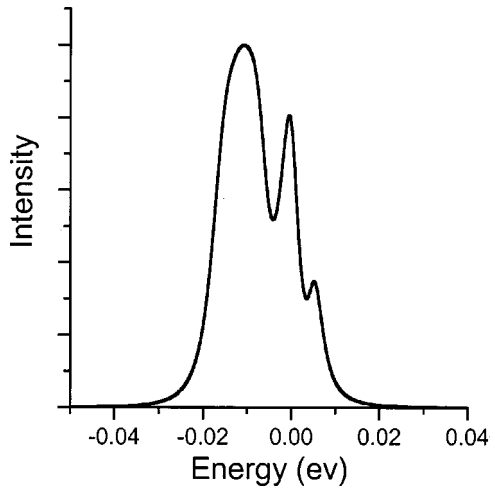

FIG. 2. Numerical calculation of a TFWM spectrum using the MOBE's, with both EID and EIS present.

by perturbation pathways that do not contribute to the signal, for example the population due to either pulse alone. Although these populations do not contribute to the signal, they must be included in the population when determining the dephasing rate that results in the decay of the TFWM signal. If they are calculated separately and included in the population used to calculate the dephasing rate between pulses, and after the second pulse, then the intuitive result that the decay of the TFWM depends on excitation density is obtained. Calculating to higher order in perturbation does not remedy this shortcoming, thus we conclude that this is a fundamental failure of perturbation theory. In the case of EID, it is relatively straightforward to correctly adjust the decay rates. In the case of EIS, it is more difficult, so we choose instead to numerically solve the MOBE, which allows us to include finite pulse width effects and treat EID and EIS correctly.

In Fig. 2, we show the numerical solutions to the MOBE's, which clearly exhibit a split peak, similar to that observed in the experiment. For these results, the local field, EIS, and EID were included. The numerical calculations are based on performing a spatial Fourier expansion in the paraxial approximation of the density-matrix elements and the electric field (both incident and generated). The spatial Fourier expansion is purely a tool to facilitate numerical calculation of the TFWM signal in a flexible way. Specifically, we write the electric field as

$$E(r,t)=\tfrac{1}{2}[\varepsilon(r,t)e^{+i\omega t}+\varepsilon^{*}(r,t)e^{-i\omega t}],$$

$$\varepsilon(r,t)=\sum_{s}\ e_{s}(t)e^{-i\mathbf{K}r}e^{-is\Delta\mathbf{k}r}, \tag{4}$$

and the density-matrix elements in the rotating frame as

$$\rho_{22}=\frac{1}{2}\sum_{p}\ \rho_{22(\rho)}e^{-ip\Delta\mathbf{k}r}+\hat{\rho}^{*}_{22(\rho)}e^{ip\Delta\mathbf{k}r},$$

$$\hat{\rho}_{12}=\sum_{\nu}\ \hat{\rho}_{12(\nu)}e^{-iKr}e^{-i\nu\Delta\mathbf{k}r}, \tag{5}$$

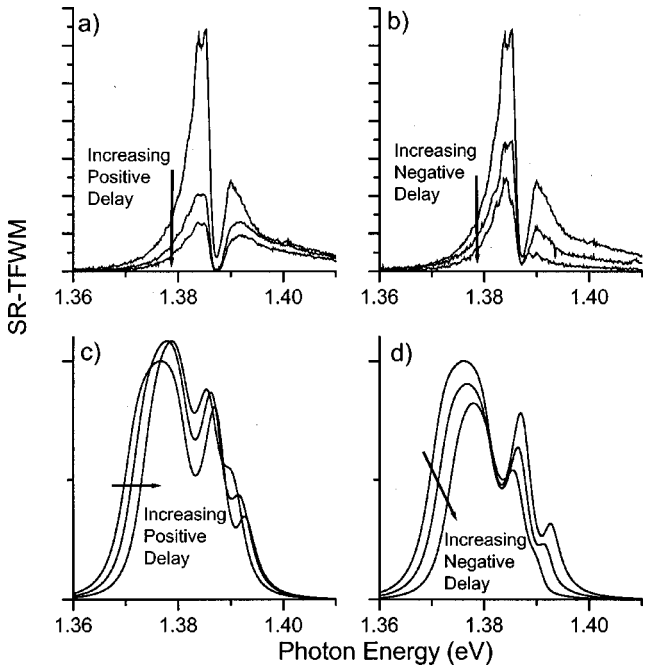

FIG. 3. Experimental data for (a) increasing delay (0, 32, and 42 fs), (b) decreasing delay (0, −10, and −35 fs), and theoretical results for (c) increasing delay (10, 50, 100, and 200 fs) and (d) decreasing delay (−10, −50, −100, and −200 fs).

where $\rho_{12}=\hat{\rho}_{12}e^{i\omega t}$ connects the rotating and nonrotating frames. Plugging these expansions into Eq. (1) yields a set of coupled differential equations that are solved numerically after being truncated spatially. We verify that the truncation does not affect the result. To simulate our two pulse TFWM experiment, we apply input fields in the $s=0$ and 1 components of the electric field. The polarization produced by the $\nu=2$ component of ρ_{12} yields the TFWM signal. Note that higher-order mixing processes are easily obtained by extending the spatial expansion. The goal of these phenomenological calculations is not a detailed fit to the data, but rather to show the essential role played by EIS. Indeed, without EIS we never see a split peak for any combination of EID and local-field parameters. These calculations are for 30-fs pulses with an area of 0.02 π, $\gamma_{ph}=300$ fs, $\gamma=10$ ps, $N\omega'=10^{4}$ ps^{-1}, $N\gamma'=10^{3}$ ps^{-1}, and $\eta=10^{2}$ (based on the perturbation analysis, these quantities can be directly compared in determining the relative contributions to the signal, by expressing the EID and EIS terms this way they are per fractional excited-state population). The calculated signal is cubic with pulse area, which is usually the criterion for being in the ''perturbative'' regime. However, in the presence of EID and EIS, this is not sufficient, but rather the magnitude of the EID and EIS parameters need to be considered as well. Simulations show that TFWM signal can saturate at pulse areas as small as 0.01 π if EID and EIS are included.[37]

The experimental and theoretical results as a function of delay show similar qualitative features (Fig. 3). As noted previously, quantum interference due to exciting continuum states causes a rapid decay of the experimental data.[23–25] This is not included in our simple theory; this theory shows a slight rise for increasing delay, while the experiment de-

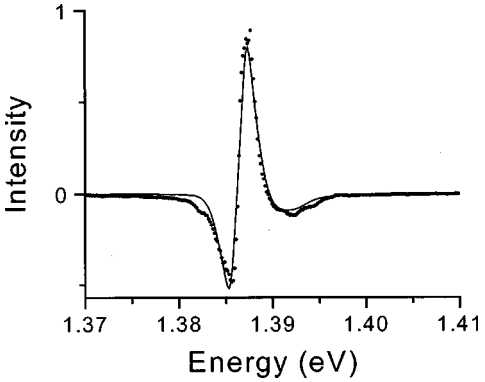

FIG. 4. Typical SR-DT curve (points) at $\tau=0$ delay, showing a strong shift, and a fit (solid line).

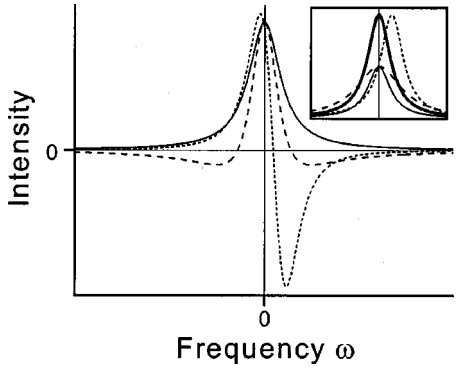

FIG. 5. The difference of two Lorentzians provides a model for SR-DT showing the processes of saturation (solid), EID (dashed), and EIS (dotted). Inset: Lorentzian curves differenced in the main figure: the reference curve (heavy), a reduced oscillator strength (solid), an increased broadening (dashed), and a positive shift (dotted).

cays immediately. For negative delay, the agreement is very good, including the faster decrease of the high-energy peak in the spectrum for both theory and experiment.

In order to show that EIS is occurring in our sample for the excitation conditions used in the SR-TFWM experiment, and estimate the relative strength compared to EID, we performed spectrally resolved differential transmission (SR-DT) measurements. The experimental setup is shown in Fig. 1(b). The probe pulse in $\mathbf{k}_2$ is attenuated by 100:1 compared to the pump pulse in $\mathbf{k}_1$. The pulse in the direction $\mathbf{k}_2$ is spectrally resolved after passing through the sample. A SR-DT spectrum is the difference in transmission with and without the pump light incident on the sample, which is proportional to the absorption per unit length in the sample. This can be written as $\Delta T/T=(I-I_0)/I_0 \propto -\Delta\alpha L$, where the transmitted intensity with and without the pump is I and I_0, respectively. Typical SR-DT data are shown in Fig. 4.

To quickly and simply understand the linear and nonlinear optical response of a homogeneously broadened system, we describe the induced polarization P as a Lorentzian,

$$P(\omega)\sim\frac{1}{2\pi}\frac{f\Gamma}{(\omega-\omega_0)^2+\frac{\Gamma^2}{4}}, \tag{6}$$

where f is the oscillator strength, Γ is the linewidth, and ω_0 is the center frequency. Any optical system will produce a nonlinear response if one or more of the three parameters f, Γ, and ω_0 depend on the intensity of the incident light.[38] The SR-DT spectra are modeled by taking the difference of two Lorentzians, where one of the parameters (f, Γ, or ω_0) is changed to represent the effect of the pump. The resulting line shapes are shown in Fig. 5. In general, a typical optical system will exhibit a superposition of the three nonlinearities. Therefore it is important to note the relative ''orthogonality'' of the curves in Fig. 5, which will enable a robust fitting procedure.

Due to the broadband excitation and the energetic proximity of the hh exciton (4 meV), the continuum state interactions have a noticeable effect on the data. When excited carriers are present, the continuum states shift to a lower energy due to band-gap renormalization.[39,40] The simple Lorentzian model for SR-DT must be corrected to account for the contribution of the continuum states. First, the linear absorption spectrum from Fig. 1(a) is fit with a pseudo-Voigt profile for the exciton plus an inverse tangent to fit the band edge. Then, the SR-DT data are fit by taking the difference of the linear absorption baseline and a spectrum with modified parameters for the pseudo-Voigt profile and band edge. From this analysis, we conclude the EID and EIS are comparable in magnitude and that saturation is negligible. Figure 4 shows typical SR-DT data for temporally coincident pulses, with a pump intensity generating $\sim 2.5\times 10^{10}$ carriers/cm^2/layer. The fit yields a shift of 1.78 meV, broadening of 0.05 meV, and a decrease in oscillator strength of 7×10^{-4}. Also apparent in Fig. 4 is a dip on the high-energy side of the exciton peak, arising from band-gap renormalization. The relative size of these fit parameters are consistent with the parameters used to calculate the spectrum shown in Fig. 2 (the overall magnitude depends on the choice of N used in the calculation). Additionally, we performed partially nondegenerate SR-DT with a spectrally narrow pump pulse tailored to overlap only the continuum and a broadband probe. These data (not shown) were strongly dominated by the shift, making the band-gap renormalization contribution more distinct.

Under broadband excitation conditions, where both the exciton and free electron-hole pairs (continuum states) are excited, a comparison of the decay of time-integrated TFWM and the width of SR-TFWM (or absorption linewidth) yields conflicting results. Specifically, if the decay of the TFWM signal as a function of delay is interpreted as being due to dephasing, the corresponding homogeneous linewidth is significantly broader than observed. This has been explained in terms of quantum interference arising from coupling between the exciton and continuum states.[23–25] Any coupling between the exciton and continuum causes rapid decay of the TFWM signal due to destructive interference. The decay does not depend on the details of the coupling between the continuum states and exciton, but it is important to know how it arises. Earlier work[24,25] only included EID, however, we observe that similar shifts of the exciton are observed in SR-DT for excitation in the continuum. This indicates that EIS also contributes strongly to the coupling. In addition,

coupling between opposite spin excitons has been studied by time resolving beats between heavy and light holes[19] and by observing Raman coherences.[41,42] The time-resolved results were well produced by a phenomenological model that included EID as the coupling mechanism.[19] We suggest that EIS should be considered here as well.

In summary, we have shown that excitation induced shifts can contribute to the coherent TFWM signal in semiconductors. Calculations provide a unique signature for the presence of EIS, which we observe. Spectrally resolved differential transmission measurements confirm the presence of EIS in our sample. Finally, we note that EIS was not considered when making a connection between the microscopic approach and the phenomenological approach,[20] which yielded some surprising correlations between the two. We suggest that the inclusion of EIS may provide a more intuitive picture.

The authors would like to acknowledge W. Stolz (Materials Science Center, Philipps-University, Germany) for providing the semiconductor sample. Funding was provided by NIST and the NSF.

*Staff member, NIST Quantum Physics Division. Email address: cundiffs@jila.colorado.edu

[1] L. Allen and J. H. Eberly, *Optical Resonance and Two-Level Atoms* (Wiley, New York, 1975).
[2] D. S. Chemla and J. Shah, Nature (London) **411**, 549 (2001).
[3] L. Schultheis, A. Honold, J. Kuhl, K. Köhler, and C. W. Tu, Phys. Rev. B **34**, 9027 (1986).
[4] L. Schultheis, J. Kuhl, A. Honold, and C. W. Tu, Phys. Rev. Lett. **57**, 1635 (1986).
[5] P. C. Becker, H. L. Fragnito, C. H. Brito Cruz, R. L. Fork, J. E. Cunningham, J. E. Henry, and C. V. Shank, Phys. Rev. Lett. **61**, 1647 (1988).
[6] T. Yajima and Y. Taira, J. Phys. Soc. Jpn. **47**, 1620 (1979).
[7] D.-S. Kim, J. Shah, T. C. Damen, W. Schäfer, F. Jahnke, S. Schmitt-Rink, and K. Köhler, Phys. Rev. Lett. **69**, 2725 (1992).
[8] S. Weiss, M.-A. Mycek, J.-Y. Bigot, S. Schmitt-Rink, and D. S. Chemla, Phys. Rev. Lett. **69**, 2685 (1992).
[9] H. Haug and S. W. Koch, *Quantum Theory of the Optical and Electronic Properties of Semiconductors* (World Scientific, Singapore, 1993).
[10] T. Ostreich, K. Schonhammer, and L. J. Sham, Phys. Rev. B **58**, 12 920 (1998).
[11] K. Leo, M. Wegener, J. Shah, D. S. Chemla, E. O. Göbel, T. C. Damen, S. Schmitt-Rink, and W. Schäfer, Phys. Rev. Lett. **65**, 1340 (1990).
[12] M. Wegener, D. S. Chemla, S. Schmitt-Rink, and W. Schäfer, Phys. Rev. A **42**, 5675 (1990).
[13] H. Wang, K. Ferrio, D. G. Steel, Y. Z. Hu, R. Binder, and S. W. Koch, Phys. Rev. Lett. **71**, 1261 (1993).
[14] Y. Z. Hu, R. Binder, S. W. Koch, S. T. Cundiff, H. Wang, and D. G. Steel, Phys. Rev. B **49**, 14 382 (1994).
[15] H. Wang, K. B. Ferrio, D. G. Steel, P. R. Berman, Y. Z. Hu, R. Binder, and S. W. Koch, Phys. Rev. A **49**, R1551 (1994).
[16] K. Bott, O. Heller, D. Bennhardt, S. T. Cundiff, P. Thomas, E. J. Mayer, G. O. Smith, R. Eccleston, J. Kuhl, and K. Ploog, Phys. Rev. B **48**, 17 418 (1993).
[17] E. J. Mayer, G. O. Smith, V. Heuckeroth, J. Kuhl, K. Bott, A. Schulze, T. Meier, D. Bennhardt, S. W. Koch, P. Thomas, R. Hey, and K. Ploog, Phys. Rev. B **50**, 14 730 (1994).
[18] J. A. Bolger, A. E. Paul, and A. L. Smirl, Phys. Rev. B **54**, 11 666 (1996).
[19] A. L. Smirl, M. J. Stevens, X. Chen, and O. Buccafusca, Phys. Rev. B **60**, 8267 (1999).
[20] K. Victor, V. M. Axt, G. Bartels, A. Stahl, K. Bott, and P. Thomas, Z. Phys. B: Condens. Matter **99**, 197 (1996).
[21] D. S. Chemla, W. H. Knox, D. A. B. Miller, S. Schmitt-Rink, J. B. Stark, and R. Zimmermann, J. Lumin. **44**, 233 (1989).
[22] G. Manzke, Q. Y. Peng, K. Henneberger, U. Neukirch, K. Hauke, K. Wundke, J. Gutowski, and D. Hommel, Phys. Rev. Lett. **80**, 4943 (1998).
[23] S. T. Cundiff, M. Koch, W. H. Knox, J. Shah, and W. Stolz, Phys. Rev. Lett. **77**, 1107 (1996).
[24] M. U. Wehner, D. Steinbach, and M. Wegener, Phys. Rev. B **54**, R5211 (1996).
[25] D. Birkedal, V. G. Lyssenko, J. M. Hvam, and K. El Sayed, Phys. Rev. B **54**, 14 250 (1996).
[26] S. R. Bolton, U. Neukirch, L. J. Sham, D. S. Chemla, and V. M. Axt, Phys. Rev. Lett. **85**, 2002 (2000).
[27] H. L. Zhou, A. V. Nurmikko, C. C. Chu, J. Han, R. L. Gunshor, and T. Takagahara, Phys. Rev. B **58**, R10 131 (1998).
[28] G. Bartels, A. Stahl, V. M. Axt, B. Haase, U. Neukirch, and J. Gutowski, Phys. Rev. Lett. **81**, 5880 (1998).
[29] T. Häupl, H. Nickolaus, F. Henneberger, and A. Schülzgen, Phys. Status Solidi B **194**, 219 (1996).
[30] B. Haase, U. Neukirch, J. Gutowski, J. Nurnberger, W. Faschinger, M. Behringer, D. Hommel, V. M. Axt, G. Bartels, and A. Stahl, J. Cryst. Growth **214**, 856 (2000).
[31] V. M. Axt, B. Haase, and U. Neukirch, Phys. Rev. Lett. **86**, 4620 (2001).
[32] V. A. Sautenkov, H. van Kampen, E. R. Eliel, and J. P. Woerdman, Phys. Rev. Lett. **77**, 3327 (1996).
[33] S. Mukamel, Annu. Rev. Phys. Chem. **51**, 691 (2000).
[34] S. Lutgen, T. Marschner, W. Stolz, E. O. Göbel, and L. Tapfer, J. Cryst. Growth **152**, 1 (1995).
[35] M. T. Asaki, C.-P. Huang, D. Garvey, J. Z. Zhou, H. C. Kapteyn, and M. M. Murnane, Opt. Lett. **18**, 977 (1993).
[36] A. Honold, L. Schultheis, J. Kuhl, and C. W. Tu, Appl. Phys. Lett. **52**, 2105 (1988).
[37] J. M. Shacklette and S. T. Cundiff, *OSA Trends in Optics and Photonics*, Vol. 74, Quantum Electr. and Laser Sci. Conf., OSA Technical Digest (Optical Society of America, Washington D.C., 2002), p. 209.
[38] S. Schmitt-Rink, D. S. Chemla, and D. A. B. Miller, Phys. Rev. B **32**, 6601 (1985).
[39] C. V. Shank, R. L. Fork, R. F. Leheny, and J. Shah, Phys. Rev. Lett. **42**, 112 (1979).
[40] J. C. Ryan and T. L. Reinecke, Phys. Rev. B **47**, 9615 (1993).
[41] K. B. Ferrio and D. G. Steel, Phys. Rev. Lett. **80**, 786 (1998).
[42] M. E. Donovan, A. Schülzgen, J. Lee, P.-A. Blanche, N. Peyghambarian, G. Khitrova, H. M. Gibbs, I. Rumyantsev, N. H. Kwong, R. Takayama, Z. S. Yang, and R. Binder, Phys. Rev. Lett. **87**, 237402 (2001).